2021-08

# Comparison of blue and green water fluxes for different land use classes in a semi-arid cultivated catchment using remote sensing

Msigwa, Anna

Elsevier

https://doi.org/10.1016/j.ejrh.2021.100860

Journal of Hydrology: Regional Studies 36 (2021) 100860

Contents lists available at ScienceDirect

Journal of Hydrology: Regional Studies

journal homepage: www.elsevier.com/locate/ejrh

# Comparison of blue and green water fluxes for different land use classes in a semi-arid cultivated catchment using remote sensing

Anna Msigwa [a,b,*], Hans C. Komakech [a], Elga Salvadore [b,c], Solomon Seyoum [b,c], Marloes L. Mul [c], Ann van Griensven [b,c]

[a] The Nelson Mandela African Institution of Science and Technology, Arusha, Tanzania
[b] Vrije Universiteit Brussels, Belgium
[c] IHE Delft Institute for Water Education, Delft, the Netherlands

ARTICLE INFO

*Keywords:*
Evapotranspiration
Water fluxes
Water management
Land Use Land Cover

ABSTRACT

*Study area:* Kikuletwa catchment, Upper Pangani River Basin, Tanzania.
*Study focus:* This study compared yearly blue and green water fluxes using four different methods: Senay's method (SN) (Senay et al., 2016), van Eekelen method (EK) (van Eekelen et al., 2015), the Budyko method (Simons et al., 2020) and the Soil Water Balance (SWB) model (FAO and IHE Delft, 2019). The yearly blue and green water fluxes of different Land Use Land Cover (LULC) classes were estimated using an ensemble of seven global remote sensing-based evapotranspiration products (Ensemble ET) and the CHIRPS rainfall dataset. The Ensemble ET was created from seven global RS-based surface energy balance models (GLEAM, CMRS-ET, SSEBop, ALEXI, SEBS, ETMonitor and MOD16).
*New hydrological insights:* Our study found that the EK method was able to map blue and green water fluxes with realistic results for irrigated and non-irrigation cultivated areas. Budyko and SWB gave too high blue water fluxes for the non-irrigated agricultural areas, whereas the Budyko and SWB models were not able to show a clear difference in blue-water fluxes in irrigated versus non-irrigated areas. On the other hand, the SN method estimated no blue water fluxes in more than half of the identified irrigated areas.
Three of the four methods estimate the highest blue water fluxes (318–582 mm/y) in forested areas, while the SWB model estimates the highest blue water fluxes in irrigated banana and coffee (278 mm/y). Overall, we conclude that the EK method yielded the most realistic spatial pattern of blue-water fluxes when compared to the irrigated land use map, whereas SWB could be considered after further calibration if higher temporal data resolution (e.g. monthly) is required.

## 1. Introduction

Water is an increasingly scarce resource globally and life and livelihoods are threatened due to lack of access to safe and affordable water for domestic, agriculture and industrial uses. Agriculture and food production are by far the largest consumer of available blue water resources (70 % of total water withdrawals globally, FAO, 2017). Hereby blue water is defined as the water situated in rivers, lakes, wetlands and shallow aquifers. However, these estimates of water consumption do not take into consideration the direct use of

* Corresponding author at: Department of Hydrology and Hydraulic Engineering, Vrije Universiteit Brussel, Pleinlaan 2, 1050, Brussels, Belgium.
*E-mail address:* anna.msigwa@nm.aist.ac.tz (A. Msigwa).

https://doi.org/10.1016/j.ejrh.2021.100860
Received 10 August 2020; Received in revised form 14 May 2021; Accepted 18 May 2021
Available online 20 July 2021

rainfall (green water) in agricultural food production (Luo and Tao, 2016). Green water is the water stored in the root zone (soil moisture) as the result of precipitation and it can be used in rainfed and irrigated agriculture. It is important to make this distinction as interventions to improve the efficiency of water use in agriculture, needed to deal with the looming water scarcity, vastly differ between blue and green water uses (Hoekstra, 2019). Further, water resources management can benefit from estimating blue and green water fluxes aggregated by Land Use Land Cover (LULC) types, for example, to develop water budgets, monitor aquifer depletion, monitor water rights compliance and to optimize irrigation (Anderson et al., 2012). Since this data cannot be measured directly in the field, several methods have been developed to estimate blue and green water fluxes, however, these methods have not been compared or evaluated systematically.

Most of the methods have been applied to croplands from regional scale (Chukalla et al., 2015; Nouri et al., 2019) to global scale (Hoekstra et al., 2011; Liu and Yang, 2010). Van Eekelen et al. (2015) and Velpuri and Senay (2017), developed methods for assessing blue and green water fluxes for various LULCs such as natural forest, shrublands and commercial forest plantations. In particular, the last class is applicable to countries such as South Africa which lists water use of commercial forest plantations in its policies as part of streamflow reducing activities (Albaugh et al., 2013). This importance is highlighted by Van Eekelen et al. (2015), who estimated that natural forest and commercial forest plantations in the Incomati basin in South Africa consume between 391 and 433 mm/y of blue water. Similarly, Velpuri and Senay (2017) found for the United States of America that evergreen broadleaf forest is the largest blue water consumer (350 mm/year).

The methods for estimating blue and green water fluxes can be grouped into two categories: data-based approaches, and modelling approaches. Data-based approaches use rainfall (P) and evapotranspiration (ET) data sets. Senay et al. (2016) assume that in semi-arid conditions ($P < 300$ mm/year) most of the rainfall evaporates, so if ET exceeds P, irrigation water from ground or surface is applied (blue water fluxes); they state that this method is only applicable in semi-arid irrigated areas. Van Eekelen et al. (2015), on other hand, applied an effective rainfall factor assuming not all rainfall will be stored in the unsaturated zone to be available for uptake by plants (green water fluxes). The authors applied the method for annual timescales at both catchment and field scale using both ground data and remote sensing data. Similarly, Budyko developed a simple approach for catchment scale blue and green water fluxes analysis based on climatological characteristics of the study area (Budyko, 1974) which combines data on P, ET and the aridity index ($ET_o/P$, where $ET_o$ is reference evapotranspiration).

Model-based approaches for estimating blue and green water fluxes consist of adaptations to hydrological models (Hanasaki et al., 2010; Kiptala et al., 2014), soil water balance models (FAO and IHE Delft, 2019), crop models (Chukalla et al., 2015; Karandish and Hoekstra, 2017; Nouri et al., 2019; Zhuo et al., 2016) and phenology-based models (Velpuri and Senay, 2017). Hanasaki et al. (2010) estimated blue and green water fluxes by tracing the sources of blue water from the hydrological cycle using the global water resource model H08. The blue water estimates were further categorized into three subgroups: stream flow, medium size reservoirs ($50 \times 50$ km) and non-renewable and non-local blue water. The approach assumes that irrigated cropland always receives its full irrigation water requirement, which may result in an overestimation of the blue water. Also, based on these assumptions, water withdrawal from rivers may exceed the environmental water limits. The authors therefore suggest that further validation is required.

Kiptala et al. (2014) adapted a distributed hydrological model by using remote sensing ET data as an input to improve the model performance for the upper Pangani River basin in Tanzania. By tracing blue water use from two zones (saturated and unsaturated zone), the model was able to improve in particular the dry season flow estimates on the slopes of Mt Kilimanjaro and Mt Meru where smallholder farmers are practicing dry season irrigation. In addition, the total blue water consumption for the upper Pangani was in line with the estimates from the Pangani Basin Water Board.

FAO and IHE Delft (2019) developed a pixel-based soil water balance model specifically for estimating blue and green water fluxes to be used for developing water accounting of a river basin. The model separates ET into blue and green by tracking the soil moisture balance and by determining if the ET is satisfied only from rainfall and water stored in the soil moisture, or if additional water (blue water) is required for closing the balance. Similar to Kiptala et al. (2014), the model uses remote sensing data as input and can be applied from field, catchment, regional to global scale.

Output from crop models such as AquaCrop have also been used to estimate blue and green water fluxes (Chukalla et al., 2015; Karandish and Hoekstra, 2017; Nouri et al., 2019; Zhuo et al., 2016). AquaCrop keeps track of the soil water balance over time by simulating different sources of water in the soil and flows leaving the soil. The model can simulate various degrees of water supply, going from rain-fed, supplementary irrigation to deficit and full irrigation. The crop model considers the contribution of the capillary rise from shallow groundwater into the soil. Chukalla et al. (2015) developed a model using the AquaCrop outputs to partition blue and green transpiration and blue and green soil evaporation by tracking the pathways of rainwater and irrigation water in crop cultivation areas. The model has been applied in hyper-arid, arid, semi-arid, sub-humid and humid environments (Chukalla et al., 2015; Karandish and Hoekstra, 2017).

Finally, Velpuri and Senay (2017) used the phenology- based VegET model to estimate green water fluxes by tracking the pathways and magnitude of rainfall in the soil vegetation system, which was compared to their ET estimates using the operational simplified surface energy balance (SSEBop) model. The difference between the ET from VegET model and ET from SSEBop is then defined as blue water fluxes.

Although there is a range of approaches for estimating blue and green water fluxes, it is difficult to assess which one is more reliable, as these fluxes cannot be measured. The main objectives of the present study are therefore to compare and evaluate different methods to estimate blue and green water fluxes for a semi-arid cultivated catchment, to gain a better understanding of the disparities between blue water fluxes from different methods for agricultural land use, and to analyse blue and green water fluxes contribution of different methods for all LULC types and the possible causes of differences between the methods. Further, we evaluated the methods for estimating blue and green water fluxes for different LULC classes by comparing the spatial distribution of blue water fluxes for irrigated

and non-irrigated land use classes with local information. This comparison can serve as indirect validation of methods used in water resources assessment and for excluding certain methods from further use.

## 2. Method and data

### 2.1. Study area

The Kikuletwa catchment is one of the sub-catchments of the Pangani River Basin located in Eastern Africa (Fig. 1). The catchment covers a total area of 6,077 km$^2$. Rainfall within the catchment is bi-modal, with long rains (*Masika*) from March to June and short rains (*vuli*) from November to December. The catchment hydrological year starts from 1st October to 30th September the following year. The catchment has five tributaries: Nduruma, Themi, Usa-Kikuletwa, Sanya-Kware, Kikafu -Karanga rivers, whereby three of the tributaries (Nduruma, Themi, and Usa-Kikuletwa rivers) have recently turned ephemeral due to increased water consumption (Komakech, 2013). The water resources of the Kikuletwa catchment are characterized by the occurrence of springs originating along the slopes of Mt. Meru and Mt. Kilimanjaro. The largest springs are Chemka, Rundugai and Kware springs, providing 90 % of the water during the dry season. Kikuletwa river is one of the two large rivers discharging into Nyumba ya Mungu Dam (PBWO/IUCN, 2006). The primary water uses in the catchment are agriculture by small-scale farmers practicing supplementary and full-scale irrigation on the slopes of Mt Meru and Mt Kilimanjaro, mining, domestic water uses for the main cities (Arusha and Moshi), large scale commercial farms, tourist facilities and pastoralists. Increased population has led small scale farmers to expand their lands and irrigation systems, hence using more water for irrigation to supplement rainfall (Komakech and van der Zaag, 2013). As a result, some sections of the main Kikuletwa River have changed from perennial to ephemeral rivers (Komakech, 2013)

### 2.2. Data

#### 2.2.1. LULC maps

Three LULC maps were created using Landsat 8 (30 m resolution) images from three months (March, August and October 2016) respectively representing the three main seasons in the catchment (Msigwa et al., 2019). The March map represents the LULC during the long-wet season (*Masika*), the August map represents the dry season, and the October one the short rainy seasons (*Vuli*) (Fig. 2). Additional information such as crop calendar, site visits and farmers' interviews were used for developing the detailed seasonal LULC maps. The crop calendar and site visits were used to identify the crop types. Twenty land use classes were identified in the wet season, and 19 classes were identified for the dry and short rainy seasons. There are four main irrigated crop groups in the Kikuletwa catchment: sugarcane, banana and coffee, mixed crops and banana, coffee and maize (see also Kiptala et al., 2013). The details of how the LULC maps were created and validated can be found in Msigwa et al. (2019).

#### 2.2.2. Rainfall maps

Although several spatial rainfall sources are available for the study area, we selected the data from Climate Hazards Group Infrared

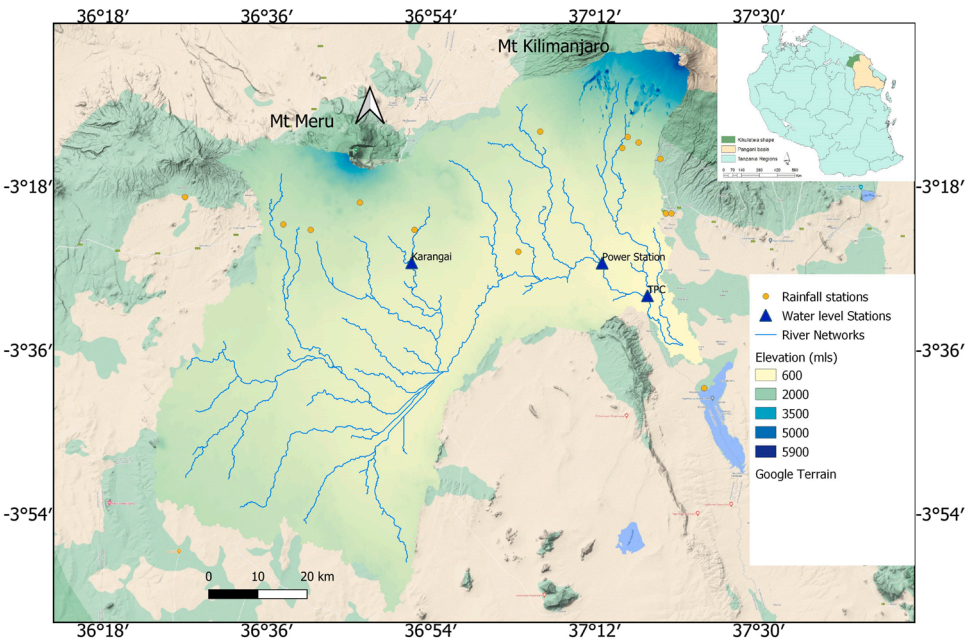


**Fig. 1.** Location and main features of Kikuletwa catchment.

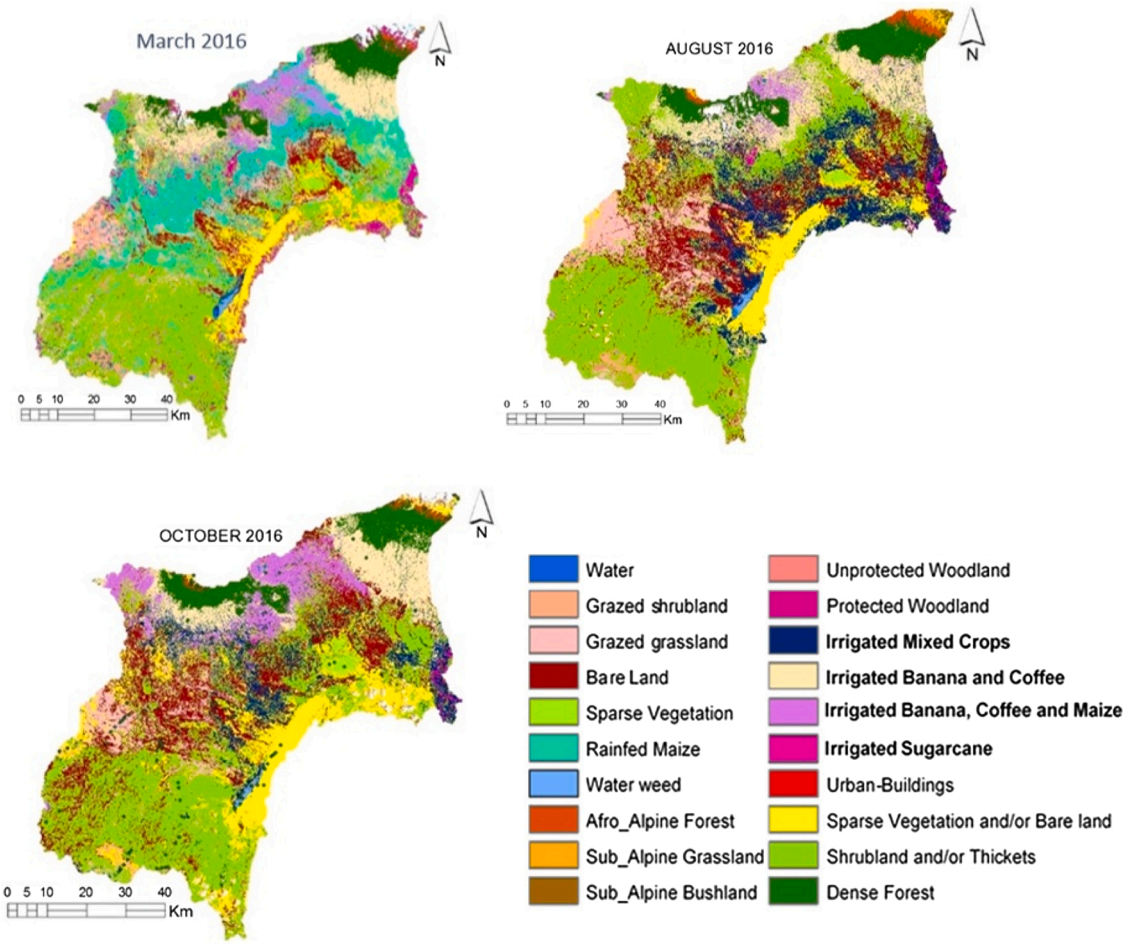


**Fig. 2.** Spatial distribution of LULC classes for the long rainy season (March) dry season (August) and short rainy season (October) in the Kikuletwa catchment (Msigwa et al., 2019).

Precipitation with Station data (CHIRPS) based on the comparative assessment done by Gebrechokos et al. (2018) in East Africa. The study showed that CHIRPS outperformed the other rainfall products (African Rainfall Climatology Version 2 [ARC2], Observational-Reanalysis Hybrid [ORH], and Regional Climatic Models [RCMs]) with a good performance in capturing daily rainfall characteristics such as number of wet days (−0.17 % deviation), total rainfall (−4.5 % deviation), average daily rainfall (−7.7 % deviation), amounts of wet periods (−17 % deviation), and duration of wet (−13.4 % deviation) and dry periods (−17.6 % deviation) over 21 validated areas including Tanzania (Gebrechorkos et al., 2018). CHIRPS is a quasi-global (50 °S–50 °N), higher resolution (0.05°), daily, pentanal and monthly dataset. It uses the Tropical Rainfall Mission Multi-satellite precipitation analysis version 7 (TMPA 3B42v7) to calibrate global Cold Cloud Duration (CCD) rainfall estimates and interpolated gauge products (Funk et al., 2015; Huffman et al., 2007).

Before using the data for our analysis, we evaluated the CHIRPS dataset with data from fifteen rainfall stations at different elevations between 696-2,000 m within and around the Kikuletwa catchment. The NashSutcliffe Efficiency coefficient (NSE) and Goodness of fit ($R^2$) were computed to compare the monthly CHIRPS rainfall estimates and measured rainfall for each station.

### 2.2.3. *Reference evapotranspiration maps*

Reference evapotranspiration ($ET_o$) was calculated from the FAO Penman-Monteith equation for standard 12 cm grass (Allen et al., 1998) using the weather data from Global Land Data Assimilation System (GLDAS; Rodell et al., 2004) and radiation data from CFSR (National Center for Atmospheric Research, 2017). The method has been applied successfully under a wide range of climate conditions (Al Zayed et al., 2016; Alemayehu et al., 2017; Autovino et al., 2016; Oweis et al., 2000).

$$ET_o = \frac{0.408(R_n - G) + \gamma \frac{900}{T-273} u_2 (e_s - e_a)}{\Delta + \gamma(1 + 0.34u_2)} \quad (1)$$

where

$ET_o$ reference evapotranspiration [mm $day^{-1}$],
$R_n$ net radiation of the crop surface [MJ $m^{-2}$ $day^{-1}$],
G soil heat flux [MJ $m^{-2}$ $day^{-1}$], is considered to be zero (Anamdranistakis et al., 1997; Sauer and Horton, 2015)
T air temperature at 2 m height [°K],
$u_2$ wind speed at 2 m height [m $s^{-1}$],
$e_s$ saturation vapour pressure [kPa],
$e_a$ actual vapour pressure [kPa],
$e_s$ - $e_a$ vapour pressure deficit of the air [kPa],
$\Delta$ slope vapour pressure curve [kPa $°C^{-1}$],
$\gamma$ psychrometric constant [kPa $°C^{-1}$].

#### 2.2.4. Actual evapotranspiration maps

The actual ET maps used in the Kikuletwa catchment are derived from an ensemble ET product developed by IHE Delft using seven Remote Sensing-based global-scale ET products (IHE Delft, 2020). All the ET products are based on multi-spectral satellite measurements and surface energy balance models: Global Land Evaporation Amsterdam Model (GLEAM) (Miralles et al., 2011), CSIRO MODIS Reflectance-based Evapotranspiration (CMRS-ET) (Guerschman et al., 2009), Operational Simplified Surface Energy Balance (SSEBop) (Senay et al., 2013), Atmosphere-Land Exchange Inverse Model (ALEXI) (Anderson et al., 2007), Surface Energy Balance System (SEBS) (Su, 2002), ETMonitor (Hu and Lia, 2015) and MODIS Global Terrestrial Evapotranspiration Algorithm (MOD16) (Mu et al., 2011). The ET maps produced by IHE Delft have a resolution of 250 × 250 m at a monthly scale. The detailed information on the ET products description and method are found in Hugo et al. (2019).

The ET product is evaluated for the study area by comparing the basin water balance at three gauged stations - Karangai, Kikuletwa Power Station (KPS) and Tanzania Plantation Company (TPC) over a period of six years (2008–2013). Fig. 1 shows the location of the three stations. The principle of water balance for the estimation of ET has been used in the past to validate remote sensing ET for basin or sub-basin level (Simons et al., 2016; Velpuri et al., 2013; Weerasinghe et al., 2020). The general water balance equation (Eq. (2)) for the three sub-catchments was used.

$$ET_{WB} = P - Q - \Delta S/\Delta t \tag{2}$$

where P, Q, and $\Delta S/\Delta t$ are the annual catchment precipitation, runoff, and change in storage per year respectively. The analysis from Gravity Recovery and Climate Experiment (GRACE) which provides estimates of the total water storage anomalies (TWSA) which also includes groundwater storage change (Ramillien et al., 2008), shows that the storage change in the Kikuletwa catchment is less than 4% of the rainfall surplus. Hence, the change in storage was assumed to be 0 ($\Delta S/\Delta t = 0$), and therefore P-ET should be equal to Q at the downstream end of the catchment (Simons et al., 2016).

### 2.3. Blue and green water fluxes estimation methods

This section briefly describes the methods used for estimating blue and green water fluxes from the total ET. The methods have been applied to the Kikuletwa catchment at an annual temporal resolution. The hydrological years from 2011 to 2014 were chosen for the comparison of blue and green water fluxes. Four methods are considered in this study, namely: SN (Senay et al., 2016), EK (van Eekelen et al., 2015), Budyko method (Simons et al., 2020) and Soil Water Balance method -SWB (FAO and IHE Delft, 2019).

#### 2.3.1. SN method

The SN method (Senay et al., 2016) estimates blue water consumption as the differences between mean annual precipitation and mean annual actual evapotranspiration (ET-P). The method assumes that when ET exceeds P, the exceeding amount is due to an additional source of water supply. The studied region must be semi-arid with rainfall not exceeding 300 mm/year as the method assumes that Q and $\Delta S/\Delta t$ are negligible (Senay et al., 2016). Most of the precipitation is lost to evaporation, leaving a negligible amount for runoff. Eqs. (3) and (4) show how the blue and green water fluxes ($ET_{blue}$ and $ET_{green}$) are estimated from total ET.

$$ET_{blue} = ET_{total} - P \tag{3}$$

$$ET_{green} = ET_{total} - ET_{blue} \tag{4}$$

#### 2.3.2. EK method

The EK method (van Eekelen et al., 2015) expresses the total ET as the sum of $ET_{blue}$ and $ET_{green}$ (Eq. (4)). Van Eekelen et al. (2015) assumes that ET in rainfed agro-ecosystem is mostly $ET_{green}$ and this information can be used to estimate $ET_{green}$ in irrigated areas. To normalize for precipitation, a ratio is calculated by dividing $ET_{green}$ over P for the rainfed areas ($F_{ET/P}$). To take into account that not all the annual rainfall infiltrates and is stored in the unsaturated zone for uptake by the roots (Eq. (5)). The blue water ($ET_{blue}$) is then the difference between the total ET and $ET_{green}$

$$ET_{green} = F_{ET/P} \times P \tag{5}$$

The map of $F_{ET/P}$ was determined using maps of ET and P of rainfed agro-ecosystem LULC classes. The analysis to obtain the $F_{ET/P}$ map was obtained based on an analysis using five years (2010–2014) of ET and P maps of the Kikuletwa catchment. Since the map of

$F_{ET/P}$ applies to selected rainfed land use class only, the $F_{ET/P}$ fraction ratio map is spatially interpolated using the average $F_{ET/P}$ values from surrounding areas that are known to be rainfed. The rainfall map is used together with an interpolated $F_{ET/P}$ map to estimate $ET_{green}$.

### 2.3.3. Budyko method

The Budyko method (De Boer, 2016), uses the Budyko curve to split ET into $ET_{green}$ and $ET_{blue}$. The Budyko curve, plots the ratio of ET to P as a function of the ratio of $ET_o$ to P (∅), also known as aridity index (Eq. (6); Budyko, 1974; Poortinga et al., 2017).

$$\frac{ETgreen}{P} = \left[\varnothing \tanh\left(\frac{1}{\varnothing}\right) * (1 - exp^{\varnothing})\right] \hat{0}.5 \tag{6}$$

where $\varnothing = \frac{ETo}{P}$

The concept is illustrated in Fig. 3, which shows the relation of ET, $ET_o$ and P for all data points in the Kikuletwa catchment as well as the Budyko curve. Values plotted below the Budyko curve indicate rainfed landscapes, whereas values plotted above the line indicate irrigated landscape.

The Budyko method was developed for applications at a basin scale (not at pixel level) and for long term analysis. We therefore computed the split between $ET_{blue}$ and $ET_{green}$ on a monthly time scale but then aggregated the results at an annual scale (hydrological years from 2011 to 2014). In our Python implementation of the method, we introduced two assumptions: (1) if rainfall is sufficient, $ET_{green}$ should account for a least 10 % of the total ET, (2) the $ET_{green}$ is a function of rainfall, and rainfall from previous months can be used in the computation of $ET_{green}$ of the current month based on the land use type (retention capacity). To take this second point into account, we used a moving average length (in months) as a function of land use type (Table 1). When we calculated $ET_{green}$ in January in cropped areas, for example, we took into account the rainfall (and $ET_o$) for December and January for computing Eqs. (6) and (4).

### 2.3.4. Soil water balance model

The soil water balance model used in this study is a pixel-based vertical water balance model which computes blue and green water fluxes (FAO and IHE Delft, 2019). The total *ET* is initially subtracted from the soil moisture supplied by rainfall ($S_{green,\ t}$). When $S_{green,\ t}$ is insufficient for *ET*, the difference will be supplied by surface or groundwater uptake. $ET_{green}$ becomes the amount which can be supplied by the soil moisture, whereas the difference will become $ET_{blue}$ (see Eqs. (7) and (4)). Fig. 4 shows the main flows and fluxes in the soil water balance model. The inputs of the model include: precipitation, actual evapotranspiration, interception, LULC map, root depth and saturated water content from HiHydroSoil (A High-Resolution Soil Map of Hydraulic Properties, De Boer, 2016). We computed the split between $ET_{blue}$ and $ET_{green}$ on a monthly time scale but then aggregated the results to annual values of hydrological year from 2011–2014.

$$ET_{green} = \text{if}\left(S_{green,t} > ET,\ ET,\ S_{green,t}\right) \tag{7}$$

where the soil moisture ($S_{green,t}$) is computed as the soil moisture storage at the end of the previous timestep ($S_{green,t-1}$) plus the effective rainfall (*P-I*) minus recharge ($R_{green}$) and surface runoff ($Q_{sro,\ green}$) (Eq. (8)).

$$S_{green,t} = S_{green,t-1} + P - I - R_{green} - Q_{sro,\ green} \tag{8}$$

where the surface runoff ($Q_{sro,green}$) is calculated using an adjusted version of the Soil Conservation Service runoff method. The adjusted version replaces the classical Curve Numbers with a dynamic soil moisture deficit term that better reflects the dry and wet season infiltration versus runoff behavior (Choudhury and DiGirolamo, 1998; Schaake et al., 1996). As the Curve Number method has been developed for event based runoff, we calculated $Q_{sro,green}$ on a daily basis, dividing the effective rainfall by the number of rainy days (*n*)

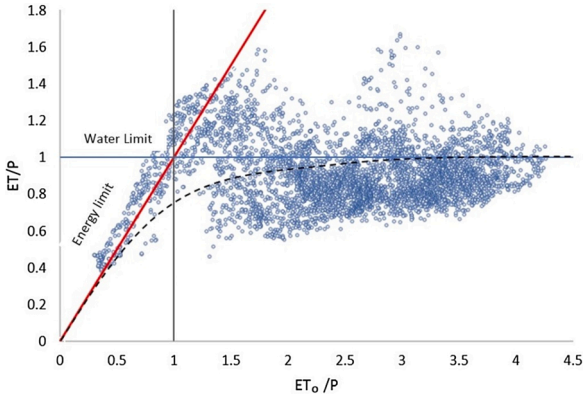


**Fig. 3.** The Budyko curve showing the relation of evapotranspiration, reference evapotranspiration and rainfall (2011-2014). The dotted line is Budyko curve, blue line is water limit and red line is energy limit line.

**Table 1**
Moving average per land use category applied in our study.

| Land use category | Moving average length (months) |
|---|---|
| Crops | 2 |
| Perennial crops | 3 |
| Savanna | 4 |
| Water | 1 |
| Forest | 5 |
| Grass | 1 |
| Other | 1 |

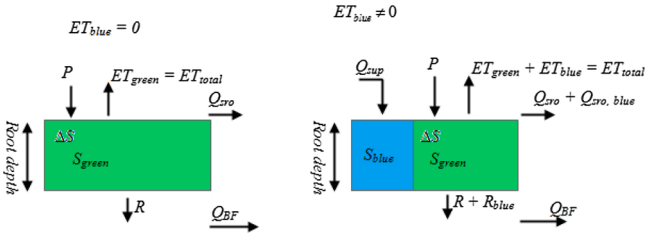


**Fig. 4.** Schematic diagram representing flows and fluxes in the soil water balance model adapted from FAO and IHE Delft, (2019).

and a calibration parameter $f$ to account for the soil moisture variation due to drying up and filling up within a month. The total surface runoff for a month is then multiplied by $n$:

$$Q_{sro,\ rain} = \begin{cases} 0 & if\ P = 0 \\ \dfrac{\left(\dfrac{P-I}{n}\right)^2}{\dfrac{P-I}{n} + f\left(S_{sat} - S_{rain,t-1}\right)} * n & if\ P \neq 0 \end{cases} \quad (9)$$

where the saturated soil moisture ($S_{sat}$) is calculated by multiplying the Saturated Water Content ($\theta_{SAT}$) by the effective root depth (RD) for each land cover class estimated based on the effective root depth by Yang et al. (2016). The reader is referred to the report by FAO and IHE Delft (2019) for detailed information about the model and its application.

### 2.4. Evaluation of the four methods

It is expected that an acceptable method will have the following characteristics:

(1) It estimates low blue water fluxes for non-irrigated areas.
(2) It is able to identify blue water consumption for most of the irrigated areas.
(3) It estimates significantly higher blue water consumption for the irrigated areas than the non-irrigated and natural areas.
(4) It estimates low blue water fluxes for natural areas except for wetlands and deep-rooted forested areas.

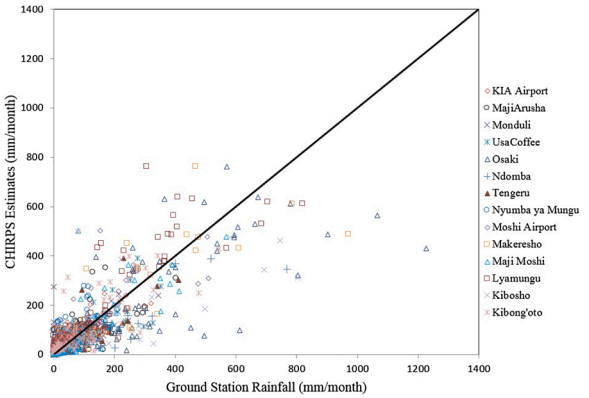


**Fig. 5.** Comparison of average monthly measured rainfall values (mm/month) and CHIRPS values (mm/month).

We evaluated the performance of the methods based on these four characteristics and by analyzing the spatial distribution of blue water fluxes using LULC maps with known irrigated areas in the Kikuletwa catchment. A one-way ANOVA with LSD (Least significant difference) Post Hoc test was performed by assuming there is no significant difference between the means of all the four methods and between each of the two methods (SN vs EK, EK vs SWB and SWB vs Budyko).

## 3. Results

### 3.1. Validation of remotely sensed P and ET in the Kikuletwa catchment

The CHIRPS monthly rainfall data showed a good agreement with station data (Fig. 5). The statistical analysis for 15 stations is presented in Table 2, whereby the overall NSE, $R^2$, slope, Pbias and Relative bias was 0.87, 0.83, 0.96, 4.6 % and 0.95, respectively.

The comparison of water balance ET ($ET_{WB}$) and the remote sensing ET showed good agreement (NSE = 0.77) for Kikuletwa Power station (KPS) which covered 86 % of the total catchment area (Msigwa et al., 2019). The overall agreement of $ET_{WB}$ and remote sensing ET is slightly lower (NSE = 0.42) for the whole catchment (at TPC station). The results of the statistical analysis between remote sensing ET and $ET_{WB}$ at the three gauged stations (Fig. 1) is summarized in Table 3.

### 3.2. Blue and green water fluxes

Average annual blue-water fluxes (mm/y) maps using the four methods were produced for the period 2011–2014 (Fig. 6). The blue water consumption ranges between 0−850 mm/year. Blue water fluxes are high in the highlands of Mount Kilimanjaro and Meru, dominated by dense forest, irrigated banana and coffee, and in irrigated sugarcane on the lower eastern side of the catchment. All four methods show lower blue water fluxes in the lowlands. In some areas in the lowlands, high blue water fluxes are obtained which are consistent with known irrigation schemes (Fig. 9), including the TPC sugarcane plantation (located in the South-East corner of the catchment).

The method by EK and SN estimated zero blue-water fluxes in more than half of the catchment area. About 76 and 51 % of the total area was identified as having no blue water consumption using the SN and EK method, respectively. In addition, the SWB and Budyko methods identified only 3 % and 0 % of the total area to have no blue water, respectively. However, according to the LULC map (Fig. 2), only 23 % of the total area are irrigated agricultural land, and 44 % of the total area dominated by LULC classes such as grazed grassland, rainfed maize and sparse vegetation is unlikely to consume blue water. Fig. 7 shows the relative contribution of blue and green water fluxes to total ET for all the methods. The spatial distribution of blue and green water fluxes significantly varies according to the method used. The Budyko method estimates that 29–59 % of the total ET in forested areas of Mount Kilimanjaro is green water fluxes, while other methods estimate green water fluxes to reach up to 80 % of the total ET. The SN method shows that in more than half of the catchment green water fluxes is equal to the total ET. The EK method can clearly distinguish between irrigated and non-irrigated areas, with blue water flux over irrigated areas being 20 % higher than for the non-irrigated areas. The Budyko method indicates that 30 % of the total ET is blue water which is consumed in more than half of the catchment area.

Fig. 8 compares the calculated blue and green water fluxes with the total ET for all LULC classes with a previous study by Kiptala et al. (2014). Across the LULC classes, the Budyko method gives the highest blue water. The LULC class with the highest blue water fluxes are dense forest followed by irrigated areas for all the methods in this study except for the SWB method where the highest blue water fluxes are found in irrigated banana and coffee.

The Budyko method estimates the lowest green water fluxes for all the LULC. The average green water fluxes for the SN and EK methods are similar in the natural LULC types. Except for forested areas, the difference in green water flux estimates between the SN and EK methods is less than 30 mm/year for most natural land cover types.

**Table 2**
Summary of monthly rainfall statistics of 15 stations in comparison with remote sensing estimates.

| STATION_NAME | X (Latitude) | Y (Longitude) | Elevation (m) | Slope | $R^2$ | NSE |
|---|---|---|---|---|---|---|
| MAJI ARUSHA | −3.38 | 36.68 | 1402 | 0.9 | 0.5 | 0.5 |
| NDO-OMBO PRIMARY SCHOOL | −3.33 | 36.77 | 1570 | 1.5 | 0.8 | 0.6 |
| USA COFFEE ESTATE | −3.38 | 36.87 | 1183 | 1.0 | 0.7 | 0.7 |
| ARUSHA MET STATION/AIRPORT | −3.37 | 36.63 | 1387 | 0.7 | 0.5 | 0.2 |
| KIBOSHO MISSION | −3.25 | 37.32 | 1478 | 1.5 | 0.7 | 0.5 |
| LYAMUNGU | −3.23 | 37.25 | 1250 | 0.8 | 0.8 | 0.7 |
| MONDULI ESTATE | −3.32 | 36.45 | 1585 | 0.9 | 0.6 | 0.5 |
| OSAKI FOREST | −3.22 | 37.28 | 1524 | 1.2 | 0.6 | 0.6 |
| TENGERU MET STATION | −3.38 | 36.87 | 1280 | 1.0 | 0.7 | 0.7 |
| MOSHI MET/AIRPORT | −3.35 | 37.33 | 813 | 0.9 | 0.7 | 0.7 |
| KILIMANJARO AIRPORT | −3.42 | 37.06 | 894 | 0.9 | 0.8 | 0.8 |
| MAJI MOSHI | −3.35 | 37.34 | 960 | 0.9 | 0.7 | 0.7 |
| KIBONG'OTO | −3.2 | 37.1 | 1379 | 0.8 | 0.5 | 0.4 |
| MAKERESHO | −3.21 | 37.26 | 1430 | 1.0 | 0.7 | 0.7 |
| NYUMBA YA MUNGU | −3.67 | 37.4 | 686 | 0.5 | 0.5 | −0.5 |

**Table 3**
Comparison statistics of remote sensing ET and $ET_{WB}$.

| Statistic | Karangai | KPS | TPC |
|---|---|---|---|
| Relative Bias | 1.1 | 1.01 | 1.01 |
| Nash-Sutcliffe Coefficient | −0.18 | 0.77 | 0.42 |
| Pearson Correlation coefficient | 0.12 | 0.90 | 0.67 |
| RMSE (mm/y) | 303 | 25 | 34 |

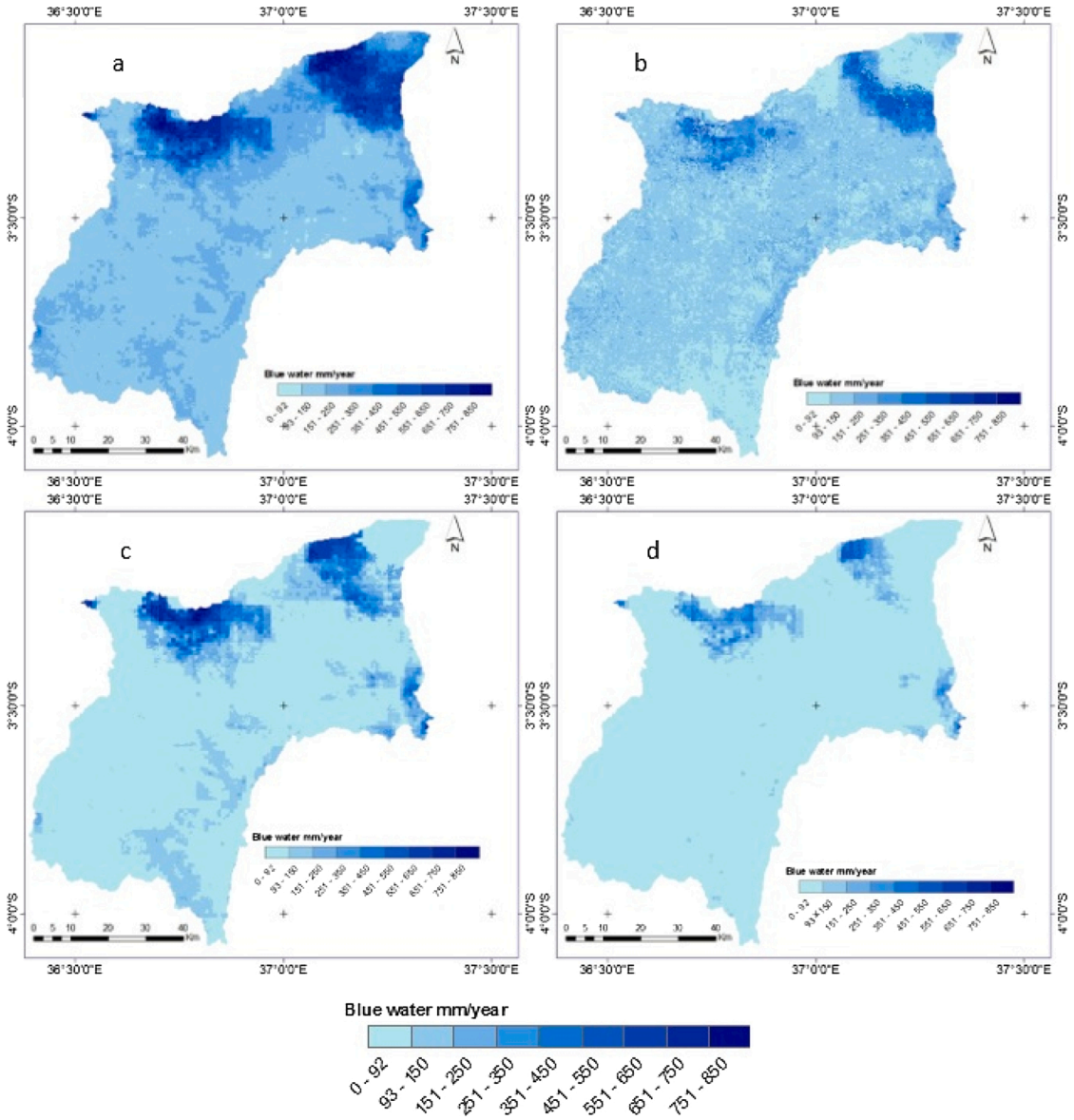


**Fig. 6.** Spatial distribution of mean blue water fluxes (2011–2014) from a) Budyko b) SWB c) EK and d) SN.

### *3.3. Blue and green water fluxes analysis of agricultural land uses*

The location of the agricultural land use classes is presented in Fig. 9, while the average annual blue and green water fluxes for the agricultural land uses from the four methods are presented in Fig. 10. The Budyko method gives the highest estimates of blue water fluxes and lowest estimates of green-water fluxes while SN method shows the lowest blue water fluxes and highest green water fluxes. For all agricultural land uses, SWB and EK methods show similar estimates of blue and green water fluxes with a difference of less than 50 mm/y except for the rainfed maize.

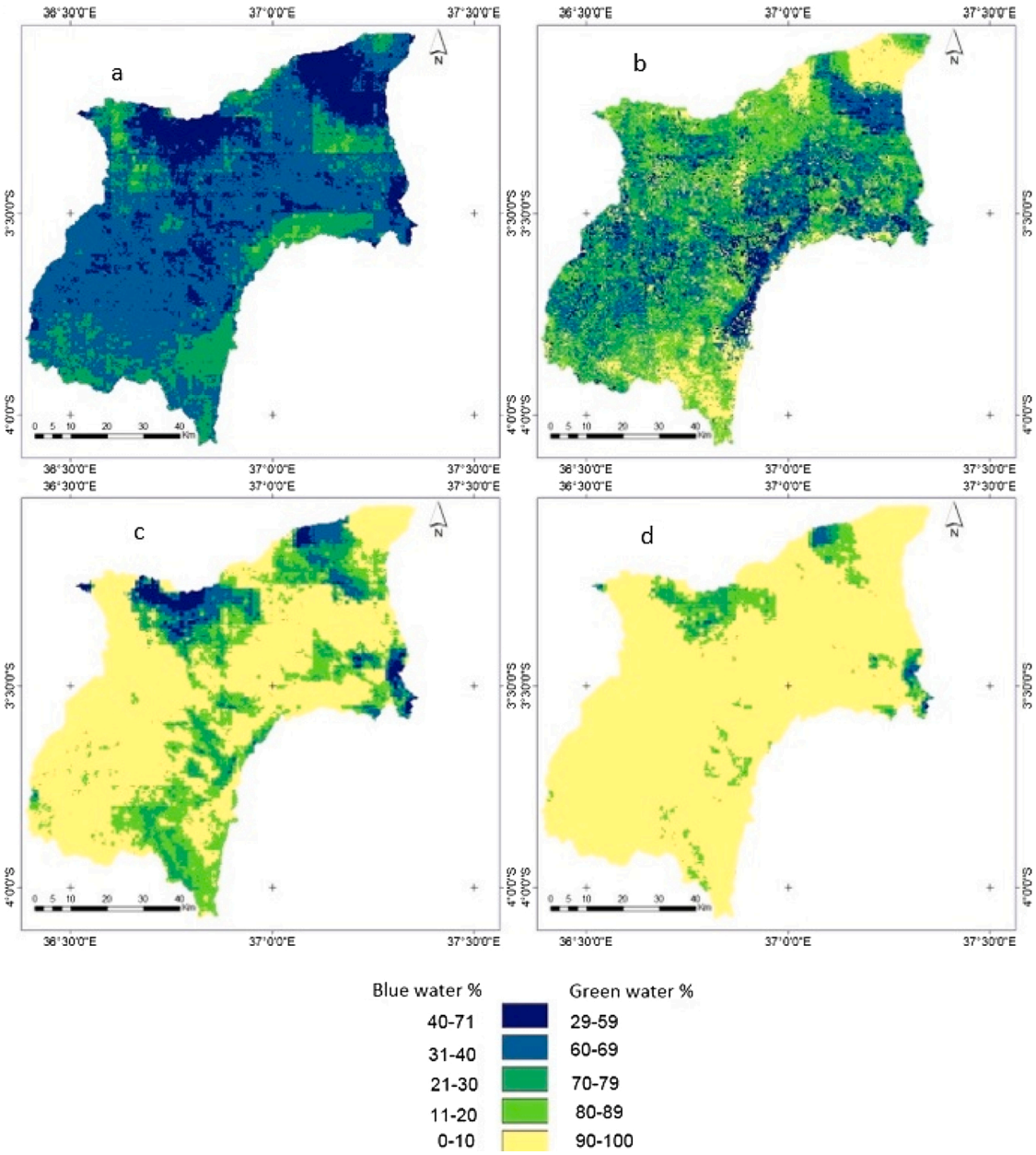


**Fig. 7.** Blue and green water fluxes contribution (%) to the total ET from a) Budyko b) SWB c) EK and d) SN.

The average blue water fluxes from the EK method in rainfed maize is low compared to the estimates of the SWB and Budyko methods, whereas the SN method shows zero blue water fluxes for rainfed maize (Fig. 8). The one-way ANOVA with LSD (least significant difference) Post hoc test of the average values shows that there is no significant difference in blue water fluxes estimated by the SN and EK methods and by the SWB and EK methods for all the LULC classes. However, there is a significant difference in the blue water fluxes estimated between the Budyko method and other methods as well as SN and SWB methods.

The average blue water fluxes estimate for irrigated sugarcane is similar in the Budyko and EK methods, whereas the blue water fluxes estimates in Budyko and other methods for the other LULC types are distinctly different. The blue water fluxes for irrigated sugarcane and non-irrigated land cover in this study significantly differs from the estimates by Kiptala et al. (2014). This may be partly due to the higher total ET estimates used in their study.

In our study, we found that the SWB method has the highest blue-water fluxes on irrigated banana and coffee (278 mm/y) while other methods showed the highest blue water fluxes in dense forest followed by the irrigated banana and coffee (Figs. 11 and 12). Kiptala et al. (2014) calculated the blue water fluxes for the Upper Pangani Basin (Kikuletwa is one of its sub-catchments) and found the highest blue water fluxes in irrigated sugarcane (466 mm/y) followed by irrigated banana and coffee (266 mm/y). However, all the

| Category | | Blue water (mm/year) | | | | | Green water mm/year | | | | | Total ET (mm/year) | |
|---|---|---|---|---|---|---|---|---|---|---|---|---|---|
| | LULC class | SN | EK | SWB | Budyko | Kiptala | SN | EK | SWB | Budyko | Kiptala | This study | Kiptala |
| Natural lands | Water | 66 | 107 | 144 | 194 | | 479 | 439 | 401 | 352 | | 545 | |
| | Grazed shrubland | 43 | 59 | 121 | 165 | | 474 | 458 | 396 | 351 | | 517 | |
| | Grazed grassland | 38 | 45 | 127 | 160 | | 400 | 393 | 311 | 278 | | 438 | |
| | Bare land | 45 | 57 | 139 | 157 | | 426 | 415 | 332 | 315 | | 472 | |
| | sparse vegetation | 44 | 52 | 125 | 150 | | 373 | 365 | 292 | 267 | | 417 | |
| | Afro Alpine forest | 47 | 181 | 92 | 352 | 115 | 915 | 781 | 870 | 610 | 1314 | 962 | 1429 |
| | Sub Alpine grassland | 10 | 120 | 134 | 329 | | 807 | 697 | 682 | 488 | | 816 | |
| | Sub Alpine bushland | 0 | 110 | 156 | 344 | | 780 | 670 | 624 | 437 | | 780 | |
| | Unprotected woodland | 45 | 68 | 121 | 156 | | 466 | 442 | 389 | 354 | | 510 | |
| | Protected woodland | 87 | 127 | 136 | 219 | | 559 | 519 | 510 | 427 | | 646 | |
| | Water weed | 75 | 132 | 179 | 191 | | 469 | 411 | 364 | 353 | | 543 | |
| | Urban_Buildings/Settlement | 45 | 59 | 137 | 154 | | 402 | 388 | 309 | 292 | | 447 | |
| | Sparse vegetation and/or bare land | 44 | 66 | 156 | 160 | | 449 | 427 | 336 | 332 | | 493 | |
| | Shrubland and/or Thickets | 46 | 69 | 118 | 175 | 8 | 461 | 438 | 389 | 332 | 748 | 507 | 756 |
| | Dense Forest | 318 | 453 | 183 | 582 | 129 | 988 | 854 | 1123 | 725 | 1162 | 1306 | 1291 |
| | | | | | | | | | | | | | |
| Non-Irrigated | Rainfed Maize | 0 | 5 | 79 | 96 | 15 | 282 | 277 | 203 | 187 | 735 | 283 | 750 |
| | | | | | | | | | | | | | |
| Irrigated | Irrigated Sugarcane | 204 | 274 | 215 | 292 | 466 | 543 | 473 | 532 | 455 | 569 | 747 | 1035 |
| | Irrigated mixed crops | 52 | 111 | 135 | 191 | 181 | 507 | 448 | 425 | 369 | 724 | 560 | 905 |
| | Irrigated Banana and coffee | 247 | 321 | 278 | 410 | 266 | 743 | 668 | 711 | 579 | 1064 | 989 | 1330 |
| | Irrigated Banana coffee and maize | 113 | 160 | 150 | 267 | | 663 | 616 | 626 | 509 | | 776 | |

**Fig. 8.** Average blue and green water fluxes comparison with the total ET for all LULC from this study and previous study by Kiptala et al. (2014).

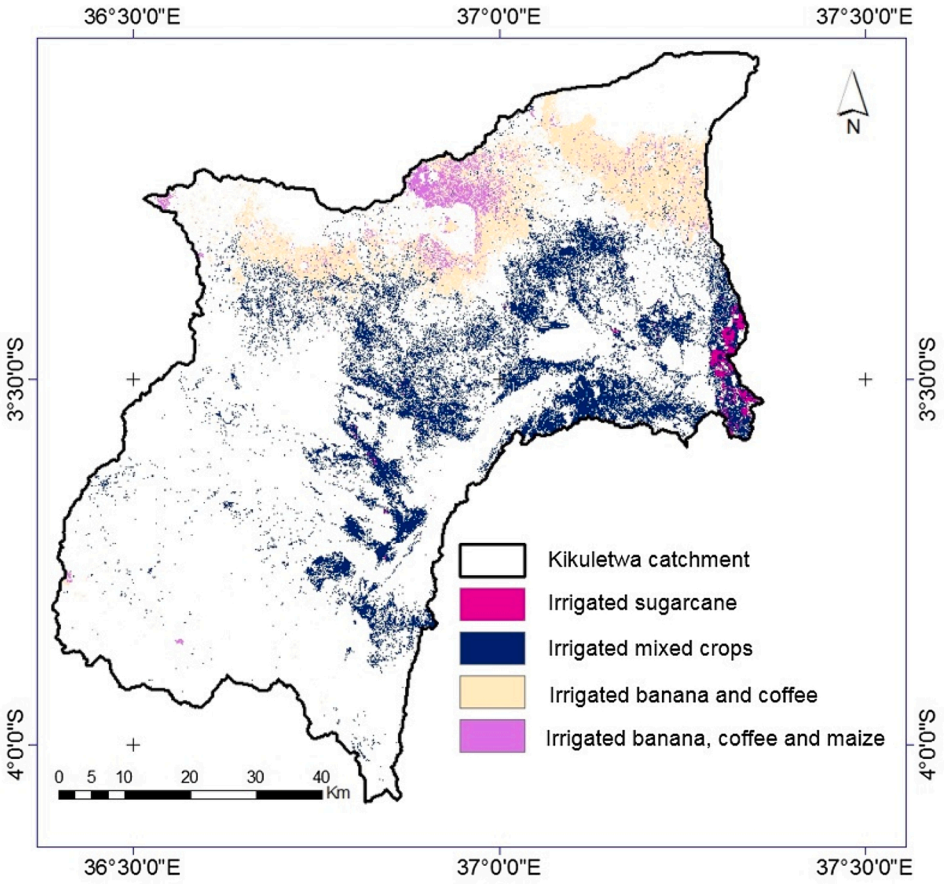


**Fig. 9.** Irrigated land use areas of Kikuletwa catchment.

methods compared in our study show different values of blue water fluxes compared to the study by Kiptala et al. (2014). The largest difference is seen in the irrigated sugarcane where the blue water fluxes are almost double the amount estimated by all methods in our study. This could be due to the fact that our catchment is a sub-catchment of the upper Pangani River basin, and thus we do not cover the entire extent of the irrigated sugarcane plantations, located in the lowlands. Also, our study used detailed land use maps of 30 m resolution and both studies used different ET products, resulting in different average and total ET for the different LULC types.

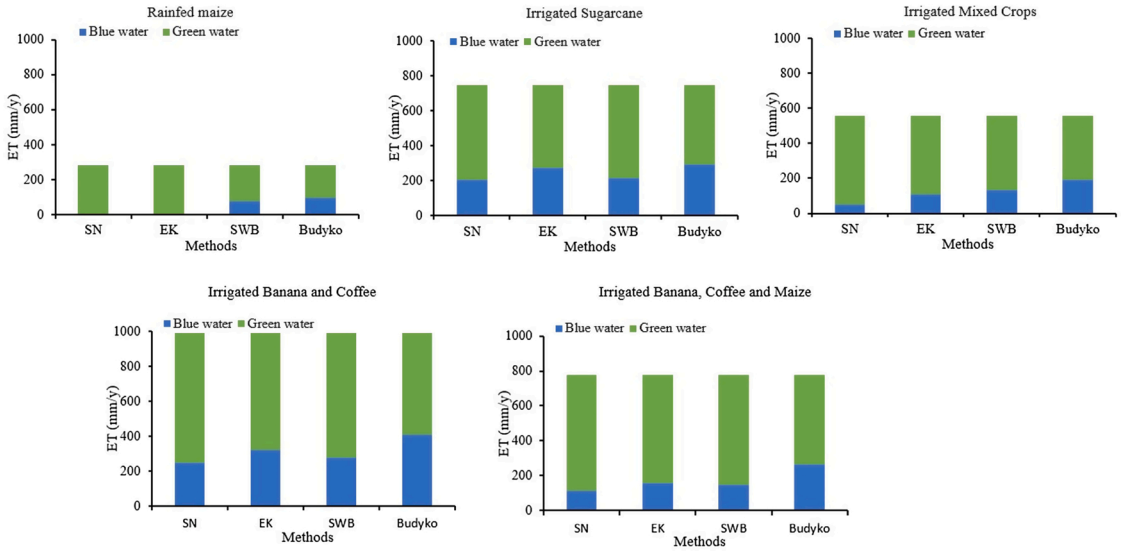


**Fig. 10.** Mean average blue and green water fluxes (mm/y) for different agricultural land uses of Kikuletwa catchment.

### *3.4. Blue and green water fluxes of natural LULC classes*

The natural LULC classes have larger variations in blue water fluxes among the different methods used in this study and that by Kiptala et al. (2014) (Fig. 8). The values from two methods (SN and EK) seem to agree in the estimation of blue water fluxes from most natural lands. Except for natural water, woodlands, and forests, blue water fluxes in all natural lands are less than 100 mm/y as estimated using both the SN and EK methods.

According to all four methods, forested areas are dependent on blue water and the blue water fluxes ranges from 180−590 mm/yr. Other studies confirm that blue water fluxes in the forested areas plays a significant role (van Eekelen et al., 2015; Velpuri and Senay, 2017). For instance, the analysis by Velpuri and Senay (2017) for different LULC classes in the United States found that the forested areas have higher blue water fluxes than other LULC classes.

### *3.5. Evaluation of the four methods*

The comparison of the methods for blue water consumption in irrigated areas, shows that generally all the methods estimate significant blue water consumption in the irrigated areas (Fig. 11). For the SN method, a significant portion of irrigated areas estimate 0 mm/y of blue water fluxes, including the lower areas in the basin, dominated by irrigated mixed crops. The EK method captures the blue water consumption in more irrigated areas compared to the SN method, whereas SWB and Budyko methods are able to capture blue water consumption in all irrigated areas.

The comparison of the methods for blue water consumption in rainfed areas shows blue water consumption in rainfed areas, for all the methods (Fig. 12). All methods estimated blue water consumption in rainfed areas, which might indicate supplementary irrigation. However, the spatial distribution and the total amount of blue water fluxes significantly differ between methods. In rainfed maize areas, the yellowish polygon in Fig. 12, only 30 % of the area indicates blue-water fluxes (<100 mm/y) according to SN and EK methods, whereas the Budyko method indicates that most areas in rainfed areas consume blue water (<100 mm/y). The SWB shows smaller areas in rainfed areas consuming blue water compared to the Budyko method.

Further, the evaluation based on irrigated versus rainfed areas shows that all the methods have higher average values of blue water fluxes in irrigated areas than the rainfed areas (Fig. 8). All methods show a significant difference between the irrigated and rainfed areas. However, the SWB and Budyko methods show higher blue water fluxes (more than 70 mm/y) in rainfed areas than the EK and SN methods.

The final evaluation was conducted based on the blue water fluxes in irrigated and non-irrigated areas. All methods estimate blue water fluxes to be higher in irrigated areas than in non-irrigated natural areas. The EK method shows the highest difference reaching 100 mm/y between the irrigated and non-irrigated natural areas.

## 4. Discussion

### *4.1. Comparison of blue-water fluxes of the four methods*

The SN method estimated blue water fluxes mostly in dense forest, irrigated areas, including banana and coffee in highland areas and sugarcane in lowland areas. The SN method has limits in its application, as the method does not perform well in areas with P > 300

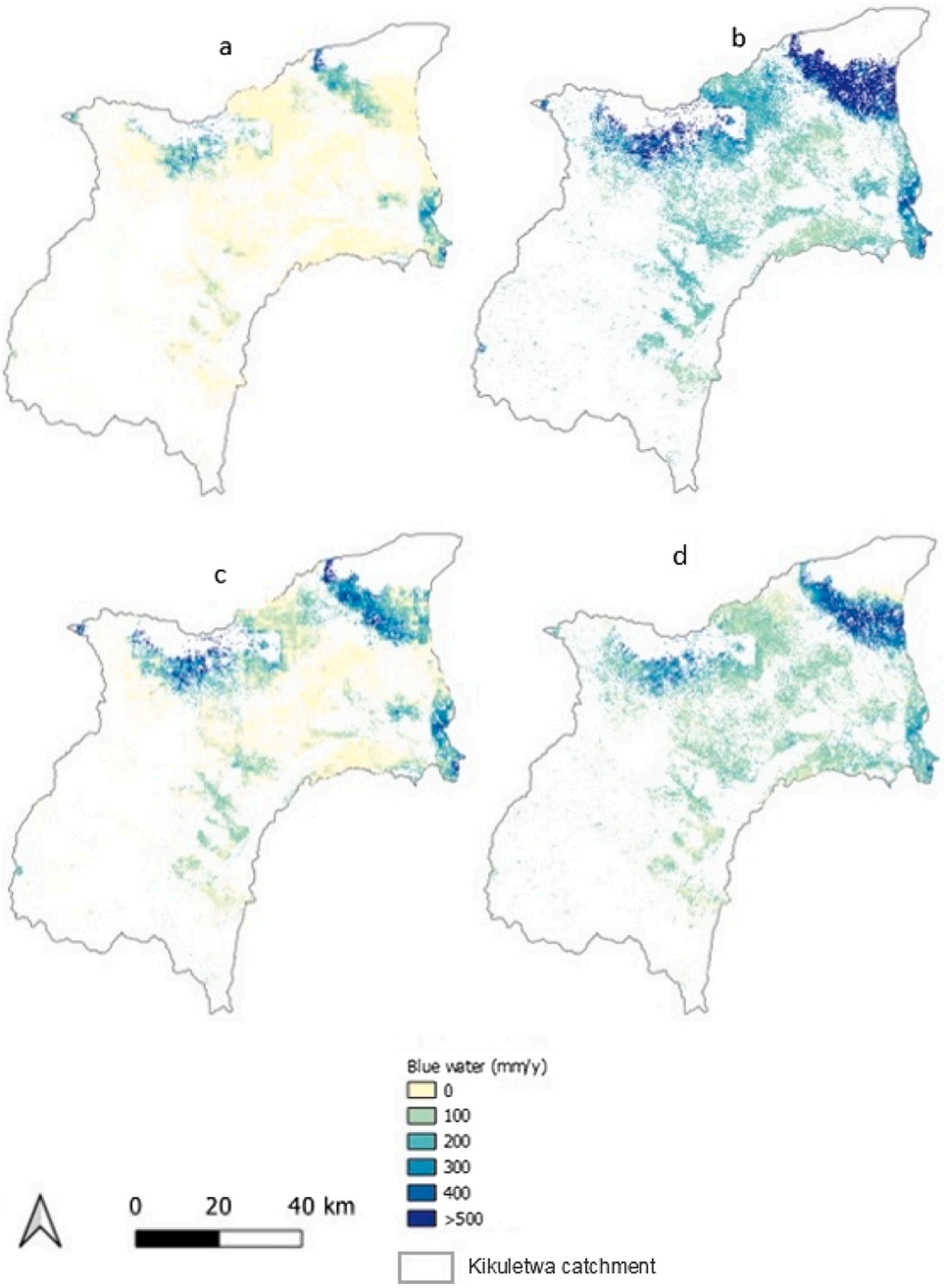


**Fig. 11.** Spatial distribution of blue water fluxes for the irrigated land use classes of Kikuletwa catchment from a) SN, b) Budyko, c) EK and d) SWB methods.

mm/year (Senay et al., 2016), which is the case for a large part of our study area. In this study, the SN method was not able to identify blue water consumption in most of the irrigated areas in the lowlands receiving average rainfall of 300 mm/year. Finally, the method clearly distinguished the irrigated from rainfed areas and non-irrigated natural areas. This is mainly due to the fact that the method is not able to identify a significant number of pixels that are irrigated (e.g. 85 % of total irrigated pixels have less than 50 mm/y of blue water fluxes). As a result, we recommend against using the method in this or similar tropical catchments with comparable characteristics.

The Budyko method was developed for basin analyses and longer time series; this study analyses only four hydrological years and estimates the blue and green water fluxes per land use types. The blue water fluxes estimates (more than 30 % of total ET) using the Budyko method is the highest for all LULC classes compared to the other methods. The blue water fluxes in the natural and rainfed areas are therefore likely to be overestimated. The method also does not distinguish a significant difference between the irrigated and

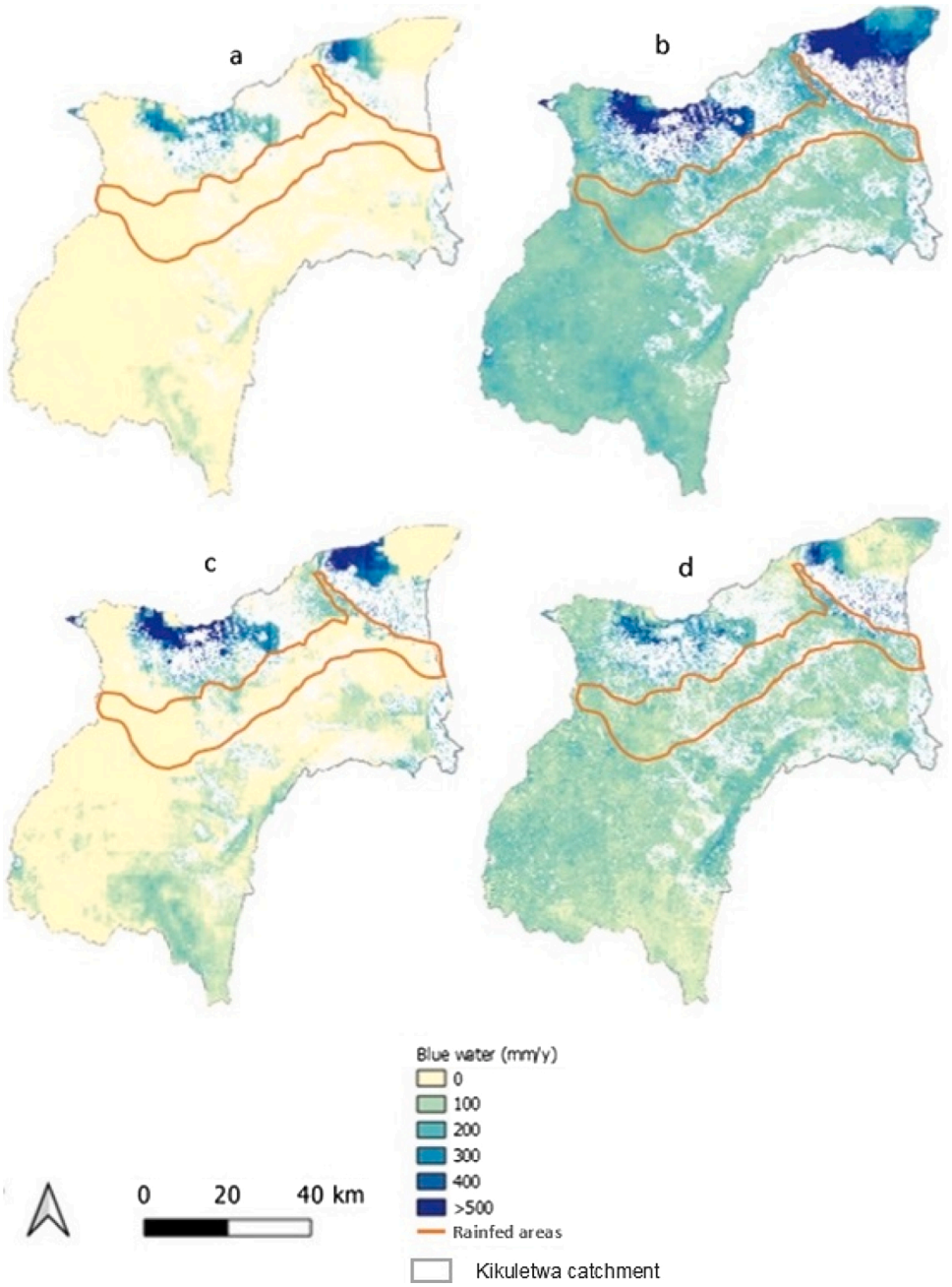


**Fig. 12.** Spatial distribution of blue water fluxes for the non-irrigated land use classes of Kikuletwa catchment from a) SN, b) Budyko, c) EK and d) SWB methods.

non-irrigated land use classes. The method is not recommended for this particular catchment and a similar analysis should be performed before the application of the Budyko method in other catchments.

The EK method was able to correctly identify irrigated areas and non-irrigated areas based on the blue water fluxes estimate. Visual evaluation shows that the spatial patterns of blue water fluxes have a strong resemblance to the irrigated land use locations. About 51 % of the total area, which mainly represents non-irrigated areas, shows no blue water consumption. The blue water fluxes estimated for the forested area were 452 mm/y (35 % of the ET) and seem to be overestimated. The forested areas in the catchment receive the maximum rainfall of 2000−2500 mm/yr. As a result, there is sufficient green water available for forested ecosystems, and the reliance on blue water resources is expected to be less. This dependence should certainly be lower than in the irrigated areas. However, to understand whether these forests are tapping shallow groundwater resources needs further investigation.

The SWB method shows differences in blue water fluxes between irrigated and non-irrigated pixels. The method was able to identify

non-irrigated areas that depend completely on green water, such as grasslands. However, the SWB method depends on a number of parameters, such as the available rootzone depth per land use, which could lead to over-or under-estimation of blue water fluxes in specific LULC classes. Examples are the over-estimation of blue water fluxes in rainfed and natural land use classes and under-estimation of blue water fluxes in the forested areas compared to the other three methods (SN, Budyko and EK).

We therefore recommend the use of the EK method for this catchment or other similar tropical catchments if high temporal resolution is not needed and the purpose of the analysis is mainly the identification of irrigated areas. The EK method will lead to better results when used in catchments that have exclusively rainfed areas that are known and mapped, which is needed for the estimation of the effective rainfall factor. For higher temporal resolution analyses or when no rainfed areas could be mapped, we recommend the SWB method for application but recommend further checks of the equations and calibrations to improve the estimation of parameters such as soil moisture and base flow have been implemented.

### 4.2. Limitations

The partitioning methods assessed in this study were developed for different purposes and conditions. In this study, they were applied at annual and across different LULC classes and climatological conditions, which may have influenced the results. The SN method according to Senay et al. (2016) is only applicable for semi-arid areas with rainfall less than 300 mm/y, as it assumes that all the precipitation is lost as evaporation, hence it neglects runoff and soil infiltration. Large parts of the Pangani basin receive rainfall that exeeds 300 mm/y, this is likely the reason for the underestimation of blue water consumption in the areas with high rainfall. However, surprisingly, the SN method was also not able to identify blue water consumption in the irrigated areas located in the dry lowlands. The EK method considers an effective rainfall factor to take into account runoff and infiltration, estimated from purely rainfed areas. However, most rainfed areas in the Kikuletwa catchment also use supplementary irrigation, thereby affecting the results. It is apparent that the EK method also estimates blue water consumption in rainfed and natural areas. The Budyko method presents an approach used for long time series and at basin scale, the comparison with the other methods shows that using this concept to estimate green and blue water consumption spatially does not provide good results. Finally, the SWB method requires parameterization of the root zone depth per land use class, this is currently based on values from literature. The results show under and over estimation of blue water fluxes for specific land use classes, further reviewing of the parameterization is needed to improve the results. For all methods, the temporal timescale of one year was applied, except for the SWB method which aggregated monthly values, even though irrigation is typically a seasonal activity.

The other source of the discrepancies is the input data, which is primarily from remote sensing and shows either over- or under-estimation when compared to ground measurements. For example, validation of ET data with water balance shows that, with remote sensing ET, the catchment has the best statistics values (NSE = 0.77 Pearson = 0.9, RMSE = 25 mm and Bias = 1.01) at one outlet that covers 86 % of the entire catchment, whereas comparison with the entire catchment resulted in a lower regression value of 0.42. This could be due to uncertainties in the remote sensing ET products used to create ensemble ET such as MODIS, which is proven to be inconsistent when validated with flux tower-based ET in South Africa (Ramoelo et al., 2014) but could also be related to surface-groundwater interactions that are also influenced by the irrigation. However, the catchment water balance closed at two gauged stations, including the gauge representing the whole catchment has a RMSE of 34 mm only. The rainfall data CHIRPS on average showed a good correlation of 0.83 with the ground rainfall stations. In the higher areas of Mount Kilimanjaro and Meru, there are no ground truth stations to compare with the remote sensing P. Also, the validation data had errors, including unexpected and unrealistic high values of P or water levels. However, not more than 10 unrealistic values were detected for each parameter (P and water levels). This could be due to human error since these data are manually recorded. Such errors were corrected by taking the average of the five values of the same week of the day in which the error was found. However, because the presented results used the same data, the discrepancies are due to method differences.

## 5. Conclusion

Understanding the amount of blue water use is important when managing groundwater and river water resources within a catchment or to understand the blue and green water footprint in crop production to propose ways of increasing production (Falkenmark and Rockström, 2006; Hoekstra, 2019; Hoekstra et al., 2011). However, methods for quantification of blue and green water fluxes have not been systematically compared and evaluated, especially in the tropical catchments in sub-Saharan Africa. In this study, we compared four methods for estimating blue and green water fluxes in the Kikuletwa catchment in Tanzania; SWB, EK, SN and Budyko over the period 2011–2014.

In the absence of ground data, the validation of these methods for separating blue and green water fluxes from total ET can only be done indirectly through evaluating known patterns and comparing the results of the different methods. Our study contributes to improved understanding of the fluxes of different sources of water and how well different methods estimate blue and green water fluxes in the Kikuletwa catchment, but also to highlight their general applicability and limitations. We evaluated the four methods using seasonal LULC maps that showed the known natural, irrigated and rainfed areas. A detailed seasonal LULC maps was used to identify the rainfed and irrigated agricultural areas and natural areas and was used for evaluation purposes.

At the catchment scale, the evaluated methods give similar spatial distribution of blue and green water fluxes, but their relative contribution to total ET varies based on the method used. The SN and EK methods show that more than half of the catchment is 90–100 % green water sources dependent, while according to the SWB model, only 14 % of the total pixels are green water dependent, and according to the Budyko method, the entire area shows blue water fluxes. The non-agricultural land use classes show much higher

green water dependence for all methods except the Budyko method, and the three method results are comparable with the study by Kiptala et al. (2014). Our study found that the EK method was able to map blue and green water fluxes with realistic results for irrigated, rainfed and natural areas. Budyko and SWB gave too high blue water fluxes for the rainfed areas. Neither the Budyko nor SWB model are able to clearly distinguish blue water consumption from irrigated, rainfed and natural areas since rainfed and natural areas indicated blue water consumption from these methods. On the other hand, the SN method estimates of blue water fluxes are zero in more than half of the identified irrigated areas. The EK method is a simple method that can be used for historical mapping of blue and green water fluxes in tropical catchments as the spatial distribution of blue water fluxes for the van Eekelen et al. (2015) method matches that of irrigated land use map as compared to other methods. This method shows a distinction of blue water from irrigated, natural and rain-fed land use classes.

Three of the four methods estimate the highest blue-water fluxes (318−582 mm/y) in forested areas, while the SWB model estimates the highest blue water fluxes in irrigated banana and coffee (278 mm/y). Overall, we conclude that the EK method yields the most realistic spatial pattern of blue-water fluxes as compared to irrigated land use map. The SWB could be considered when higher temporal data resolution (e.g. monthly) is needed after calibration. Overall, the results show that highland areas, which are dominated by forest, irrigated banana and coffee and irrigated banana, coffee and maize, have higher blue water fluxes than the lowland areas dominated by crops such as maize and vegetables. This is different from what is assumed by the water authorities, i.e. there is a higher blue water fluxes in the lower lands due to expansion of small-scale farming during the dry season leading to drying of rivers in the catchment.

Although the comparative results are specifically for the Kikuletwa catchment, the study demonstrates the importance of assessing the different methods for splitting ET into green and blue water fluxes. Our study areas have several climate conditions, from plain semi-arid to mountainous areas as high as 5800 m. As a result, the findings of this study can be applied to other tropical catchments. The study recommends further comparison studies to consider expanding the scale from the catchment to tropical catchments worldwide for all the LULC types.

For sustainable water resource management, information on blue and green water needs to be reliable. Not all the methods can be applied to all catchments. This was most certainly the case for a heterogeneous catchment like Kikuletwa. Hence, the methods used to estimate blue and green water fluxes need to be screened specifically per river catchment. Further research should also consider the validation of the blue water fluxes with spatial and temporal distributed ground data. Typically, global analyses of blue and green water fluxes are performed for only a few selected crops; however, we propose broadening the analysis to include other LULC types. Also, it is important that the analysis of blue and green water fluxes is conducted at high resolution (30 m or less) for cultivated catchments such as Kikuletwa due to small scale agriculture if information at farm level is needed. Our study used available 250 × 250 m resolution ET to provide estimates of average blue and green water fluxes per LULC types. The aim was to evaluate methods to be used at larger scales with readily available data and provide information for river basin water managers that are mapping blue and green water uses and users. Additionally, longer time series analyses of blue and green water fluxes are important to evaluate the trend for water management purposes.

## Funding

This work was supported by Flemish Interuniversity Council for University Development Cooperation (VLIR-UOS) through an institutional cooperation (IUC programme) with the Nelson Mandela African Institution of Science and Technology (NM-AIST), under the funded research project "Sustainable Management of Soil and Water for the Improvement of Livelihoods in the Upper Pangani River Basin", grant number ZIUS2013AP029 and the Academic Open Water Network with grant number JOINT_2019-01-16. The Authors thank the editor and the three reviewers for their helpful comments that improved this manuscript.

## Authorship statement

**Category 1:** Conceptualization: Anna Msigwa, Hans. C. Komakech, Ann van Griensven; Data collection: Anna Msigwa. Methodology: Anna Msigwa, Elga Salvadore, Solomon Seyoum.

**Category 2:** Writing (original draft): Anna Msigwa, Ann van Griensven: Writing (reviewing and editing): Anna Msigwa, Hans. C. Komakech, Ann van Griensven, Elga Salvadore, Solomon Seyoum, Marloes Mul.

**Category 3:** Approval of the version of the manuscript to be published: Anna Msigwa, Hans. C. Komakech, Ann van Griensven, Elga Salvadore, Solomon Seyoum, Marloes Mul.

## Declaration of Competing Interest

The authors report no declarations of interest.

## Appendix A. Useful links

| Data | Source |
|---|---|

(*continued on next page*)

(*continued*)

| Data | Source |
|---|---|
| GLDAS | (https://hydro1.gesdisc.eosdis.nasa.gov/dods/GLDAS_NOAH025_3H.) |
| CFRS | (https://nomads.ncdc.noaa.gov/data/cfsr/) |
| DEM | (http://www.hydrosheds.org/data/HydroSHEDS) |
| | (https://github.com/wateraccounting/watools) |
| CFSR | https://www.ncdc.noaa.gov/data-access/model-data/model-datasets/climate-forecast-system-version2-cfsv2 |
| GRACE | https://ccar.colorado.edu/grace/gsfc.html |

## Appendix B. Supplementary data

Supplementary material related to this article can be found, in the online version, at doi:https://doi.org/10.1016/j.ejrh.2021.100860.

## References


Al Zayed, I.S., Elagib, N.A., Ribbe, L., Heinrich, J., 2016. Satellite-based evapotranspiration over gezira irrigation scheme, Sudan: a comparative study. Agric. Water Manag. 177, 66–76. https://doi.org/10.1016/j.agwat.2016.06.027.

Albaugh, J.M., Dye, P.J., King, J.S., 2013. Eucalyptus and water use in South Africa. Int. J. For. Res., 852540 https://doi.org/10.1155/2013/852540.

Alemayehu, T., Van Griensven, A., Woldegiorgis, B.T., Bauwens, W., 2017. An improved SWAT vegetation growth module and its evaluation for four tropical ecosystems. Hydrol. Earth Syst. Sci. 21, 4449–4467. https://doi.org/10.5194/hess-21-4449-2017.

Allen, R.G., Pereira, L.S., Raes, D., Smith, M., 1998. Crop Evapotranspiration: Guidelines for Computing Crop Requirements, Irrigation and Drainage Paper No. 56. FAO, Rome, Italy. https://doi.org/10.1016/j.eja.2010.12.001.

Anamdranistakis, M., Liakatas, A., Alexandris, S., Aggelides, S., Kerkides, P., Rizos, S., Pouloussilis, A., 1997. Soil heat flux in the penman-montheith evapotranspiration equation. Acta Hortic. 449, 69–74. https://doi.org/10.17660/ActaHortic.1997.449.8.

Anderson, M.C., Norman, J.M., Mecikalski, J.R., Otkin, J.A., Kustas, W.P., 2007. A climatological study of evapotranspiration and moisture stress across the continental United States based on thermal remote sensing: 2. Surface moisture climatology. J. Geophys. Res. 112, 1–13. https://doi.org/10.1029/2006JD007507.

Anderson, M.C., Allen, R.G., Morse, A., Kustas, W.P., 2012. Use of Landsat thermal imagery in monitoring evapotranspiration and managing water resources. Remote Sens. Environ. 122, 50–65. https://doi.org/10.1016/j.rse.2011.08.025.

Autovino, D., Minacapilli, M., Provenzano, G., 2016. Modelling bulk surface resistance by MODIS data and assessment of MOD16A2 evapotranspiration product in an irrigation district of Southern Italy. Agric. Water Manag. 167, 86–94. https://doi.org/10.1016/j.agwat.2016.01.006.

Budyko, M., 1974. Climate and Life. Academic, New York.

Choudhury, J.B., DiGirolamo, E.N., 1998. A biophysical process-based estimate of global land surface evaporation using satellite and ancillary data I. Model description and comparison with observations. J. Hydrol. 205, 164–185. https://doi.org/10.1016/S0022-1694(97)00147-9.

Chukalla, A.D., Krol, M.S., Hoekstra, A.Y., 2015. Green and blue water footprint reduction in irrigated agriculture: effect of irrigation techniques, irrigation strategies and mulching. Hydrol. Earth Syst. Sci. 19, 4877–4891. https://doi.org/10.5194/hess-19-4877-2015.

De Boer, F., 2016. HiHydroSoil: a High Resolution Soil Map of Hydraulic Properties (Version 1.2), Report FutureWater, p. 134.

Falkenmark, M., Rockström, J., 2006. The new blue and green water paradigm: breaking new ground for water resources planning and management. J. Water Resour. Plan. Manag. 132, 129–132. https://doi.org/10.1061/(ASCE)0733-9496(2006)132:3(129).

FAO, 2017. Water for Sustainable Food and Agriculture, a Report Produced for the G20 Presidency of Germany. Rome.

FAO, IHE Delft, 2019. Water Accounting in the Litani River Basin-Remote Sensing for Water Productivity. Water accounting series, Rome.

Funk, C., Peterson, P., Landsfeld, M., Pedreros, D., Verdin, J., Shukla, S., Husak, G., Rowland, J., Harrison, L., Hoell, A., Michaelsen, J., Funk, Chris, Peterson, Pete, Landsfeld, Martin, Pedreros, Diego, Verdin, James, Shukla, Shraddhanand, Husak, Gregory, Rowland, James, Laura Harrison, A.H., J.M, 2015. The climate hazards infrared precipitation with stations - a new environmental record for monitoring extremes. Sci. Data 2, 1–21. https://doi.org/10.1038/sdata.2015.66.

Gebrechorkos, S.H., Hülsmann, S., Bernhofer, C., 2018. Evaluation of Multiple Climate Data Sources for Managing Environmental Resources in East Africa, pp. 4547–4564.

Guerschman, J.P., Van Dijk, A.I.J.M., Mattersdorf, G., Beringer, J., Hutley, L.B., Leuning, R., Pipunic, R.C., Sherman, B.S., 2009. Scaling of potential evapotranspiration with MODIS data reproduces flux observations and catchment water balance observations across Australia. J. Hydrol. 369, 107–119. https://doi.org/10.1016/j.jhydrol.2009.02.013.

Hanasaki, N., Inuzuka, T., Kanae, S., Oki, T., 2010. An estimation of global virtual water flow and sources of water withdrawal for major crops and livestock products using a global hydrological model. J. Hydrol. 384, 232–244. https://doi.org/10.1016/j.jhydrol.2009.09.028.

Hoekstra, A.Y., 2019. Green-blue water accounting in a soil water balance. Adv. Water Resour. 129, 112–117. https://doi.org/10.1016/j.advwatres.2019.05.012.

Hoekstra, A.Y., Chapagain, A.K., Aldaya, M.M., Mekonnen, M.M., 2011. The Water Manual Assessment Footprint: Setting the Global Standard.

Hu, G., Lia, L., 2015. Monitoring of evapotranspiration in a semi-arid inland river basin by combining microwave and optical remote sensing observations. Remote Sens. 7, 3056–3087. https://doi.org/10.3390/rs70303056.

Huffman, G.J., Bolvin, D.T., Nelkin, E.J., Wolff, D.B., Adler, R.F., Gu, G., Hong, Y., Bowman, K.P., Stocker, E.F., 2007. The TRMM Multisatellite Precipitation Analysis (TMPA): quasi-global, multiyear, combined-sensor precipitation estimates at fine scales. J. Hydrometeorol. 8, 38–55. https://doi.org/10.1175/JHM560.1.

Hugo, V., Espinoza-dávalos, G.E., Hessels, T.M., Moreira, D.M., Comair, G.F., Bastiaanssen, W.G.M., 2019. The spatial variability of actual evapotranspiration across the Amazon River Basin based on remote sensing products validated with flux towers. Ecol. Process. Process. 8.

IHE Delft, 2020. ET Ensemble Version 1.0 (ETensV1.0) Technical Documentation.

Karandish, F., Hoekstra, A.Y., 2017. Informing National Food and Water Security Policy through Water Footprint Assessment: the Case of Iran. https://doi.org/10.3390/w9110831.

Kiptala, J.K., Mohamed, Y., Mul, M.L., Cheema, M.J.M., Van Der Zaag, P., 2013. Land use and land cover classification using phenological variability from MODIS vegetation in the Upper Pangani River Basin, Eastern Africa. Phys. Chem. Earth 66, 112–122. https://doi.org/10.1016/j.pce.2013.08.002.

Kiptala, J.K., Mul, M.L., Mohamed, Y.A., Van Der Zaag, P., Medani, W., 2014. Modelling stream flow and quantifying blue water using a modified STREAM model for a heterogeneous, highly utilized and data-scarce river basin in Africa. Hydrol. Earth Syst. Sci. 2287–2303. https://doi.org/10.5194/hess-18-2287-2014.

Komakech, H.C., 2013. Emergence and Evolution of Endogenous Water Institutions in an African River Basin: Local Water Governance and State Intervation in the Pangani River Basin, Tanzania. CRC Press, Balkema.

Komakech, H.C., Van Der Zaag, P., 2013. Polycentrism and pitfalls: the formation of water users forums in the Kikuletwa catchment, Tanzania. Water Int. 38, 231–249. https://doi.org/10.1080/02508060.2013.791763.

Liu, J., Yang, H., 2010. Spatially explicit assessment of global consumptive water uses in cropland: green and blue water. J. Hydrol. 384, 187–197. https://doi.org/10.1016/j.jhydrol.2009.11.024.

Luo, K., Tao, F., 2016. Dynamics of green and blue water flows and their controlling factors in Heihe River basin of northwestern China. Hydrol. Earth Syst. Sci. Discuss. 1–23. https://doi.org/10.5194/hess-2016-241.

Miralles, D.G., Holmes, T.R.H., De Jeu, R.A.M., Gash, J.H., Meesters, A.G.C.A., Dolman, A.J., 2011. Global land-surface evaporation estimated from satellite-based observations. Hydrol. Earth Syst. Sci. 15, 453–469. https://doi.org/10.5194/hess-15-453-2011.

Msigwa, A., Komakech, H.C., Verbeiren, B., Salvadore, E., Hessels, T., Weerasinghe, I., van Griensven, A., 2019. Accounting for seasonal land use dynamics to improve estimation of agricultural irrigation water withdrawals. Water (Switzerland) 11. https://doi.org/10.3390/w11122471.

Mu, Q., Zhao, M., Running, S.W., 2011. Improvements to a MODIS global terrestrial evapotranspiration algorithm. Remote Sens. Environ. 115, 1781–1800. https://doi.org/10.1016/j.rse.2011.02.019.

National Center for Atmospheric Research staff, 2017. The Climate Data Guide: Climate Forecast System Reanalysis (CFSR) [WWW Document].

Nouri, H., Stokvis, B., Galindo, A., Blatchford, M., Hoekstra, A.Y., 2019. Water scarcity alleviation through water footprint reduction in agriculture: the effect of soil mulching and drip irrigation. Sci. Total Environ. 653, 241–252. https://doi.org/10.1016/j.scitotenv.2018.10.311.

Oweis, T., Zhang, H., Mustafa, P., 2000. Water use efficiency of rainfed and irrigated bread wheat in a Mediterranean environment. Agron. J. 92, 231–238.

PBWO/IUCN, 2006. The Hydrology of the Pangani River Basin. Report 1: Pangani River Basin Flow Assessment Initiative. Moshi.

Poortinga, A., Bastiaanssen, W., Simons, G., Saah, D., Senay, G., 2017. A self-calibrating runoff and streamflow remote sensing model for ungauged basins using open-access earth observation data. Remote Sens. 9, 1–14. https://doi.org/10.3390/rs9010086.

Ramillien, G., Famiglietti, J.S., Wahr, J., 2008. Detection of continental hydrology and glaciology signals from GRACE: a review. Surv. Geophys. 29, 361–374. https://doi.org/10.1007/s10712-008-9048-9.

Ramoelo, A., Majozi, N.P., Mathieu, R., Jovanovic, N.Z., Nickless, A., Dzikiti, S., 2014. Validation of global evapotranspiration product (MOD16) using flux tower data in the African Savanna, South Africa. Remote Sens. 6, 7406–7423. https://doi.org/10.3390/rs6087406.

Rodell, M., Houser, P.R., Jambor, U., Gottschalck, J., Mitchell, K., Meng, C.J., Arsenault, K., Cosgrove, B., Radakovich, J., Bosilovich, M., Entin, J.K., Walker, J.P., Lohmann, D., Toll, D., 2004. The global land data assimilation system. Bull. Am. Meteorol. Soc. 85, 381–394. https://doi.org/10.1175/BAMS-85-3-381.

Sauer, T.J., Horton, R., 2015. Soil Heat Flux, pp. 131–154. https://doi.org/10.2134/agronmonogr47.c7.

Schaake, J.C., Koren, V.I., Duan, Q., Chen, F., 1996. Simple water balance model for estimating runoff at different spatial and temporal scales. J. Geophys. Res. 101, 7461–7475. https://doi.org/10.1029/95JD02892.

Senay, G.B., Bohms, S., Singh, R.K., Gowda, P.H., Velpuri, N.M., Alemu, H., Verdin, J.P., 2013. Operational evapotranspiration mapping using remote sensing and weather datasets: a new parameterization for the SSEB approach. J. Am. Water Resour. Assoc. 49, 577–591. https://doi.org/10.1111/jawr.12057.

Senay, G.B., Friedrichs, M., Singh, R.K., Manohar, N., Velpuri, N.M., Manohar, N., 2016. Evaluating Landsat 8 evapotranspiration for water use mapping in the Colorado River Basin. Remote Sens. Environ. 185, 171–185. https://doi.org/10.1016/j.rse.2015.12.043.

Simons, G., Bastiaanssen, W., Ngô, L.A., Hain, C.R., Anderson, M., Senay, G., 2016. Integrating global satellite-derived data products as a pre-analysis for hydrological modelling studies: a case study for the Red River Basin. Remote Sens. 8 https://doi.org/10.3390/rs8040279.

Simons, G.W.H., Bastiaanssen, W.G.M., Cheema, M.J.M., Ahmad, B., Immerzeel, W.W., 2020. A novel method to quantify consumed fractions and non-consumptive use of irrigation water: application to the Indus Basin irrigation system of Pakistan. Agric. Water Manag. 236, 106174 https://doi.org/10.1016/j.agwat.2020.106174.

Su, Z., 2002. The Surface Energy Balance System (SEBS) for estimation of turbulent heat fluxes To cite this version: HAL Id : hal-00304651 The Surface Energy Balance System (SEBS) for estimation of turbulent heat fluxes. Hydrol. Earth Syst. Sci. Discuss. 6, 85–100.

van Eekelen, M.W., Bastiaanssen, W.G.M., Jarmain, C., Jackson, B., Ferreira, F., van der Zaag, P., Saraiva Okello, A., Bosch, J., Dye, P., Bastidas-Obando, E., Dost, R.J. J., Luxemburg, W.M.J., 2015. A novel approach to estimate direct and indirect water withdrawals from satellite measurements: a case study from the Incomati basin. Agric. Ecosyst. Environ. 200, 126–142. https://doi.org/10.1016/j.agee.2014.10.023.

Velpuri, N.M., Senay, G.B., 2017. Partitioning Evapotranspiration into Green and Blue Water Sources in the Conterminous United States, Scientific Reports. Springer US. https://doi.org/10.1038/s41598-017-06359-w.

Velpuri, N.M., Senay, G.B., Singh, R.K., Bohms, S., Verdin, J.P., 2013. A comprehensive evaluation of two MODIS evapotranspiration products over the conterminous United States: using point and gridded FLUXNET and water balance ET. Remote Sens. Environ. 139, 35–49. https://doi.org/10.1016/j.rse.2013.07.013.

Weerasinghe, I., Bastiaanssen, W., Mul, M., Jia, L., Van Griensven, A., 2020. Can we trust remote sensing evapotranspiration products over Africa? Hydrol. Earth Syst. Sci. 24, 1565–1586. https://doi.org/10.5194/hess-24-1565-2020.

Yang, Y., Donohue, J.R., McVicar, R.T., 2016. Global estimation of effective plant rooting depth: implications for hydrological modeling. Water Resour. Res. 52, 8260–8276. https://doi.org/10.1002/2016WR019392.Received.

Zhuo, La, Mekonnen, Mesfi M., Hoekstra, Arjen Y., Wada, Yoshihide, 2016. Inter- and intra-annual variation of water footprint of crops and blue water scarcity in the Yellow River basin (1961–2009). Adv. Water Resour. 87, 29–41. https://doi.org/10.1016/j.advwatres.2015.11.002.